JTTEE5 17:915–923
DOI: 10.1007/s11666-008-9242-9
1059-9630/$19.00 © ASM International

Residual Stresses Distribution through Thick HVOF Sprayed Inconel 718 Coatings

C. Lyphout, P. Nylén, A. Manescu, and T. Pirling

(Submitted June 13, 2008; in revised form August 20, 2008)

Residual stress buildup in thick thermal spray coatings is a property of concern. The adhesion of these coatings to the substrate is influenced by residual stresses that are generated during the coating deposition process. In the HVOF spray process, significant peening stresses are generated during the impact of semimolten particles on the substrate. The combination of these peening stresses together with quenching and thermal mismatch stresses that arise after deposition can be of significant importance. Both numerical method, i.e., Finite Element Method (FEM), and experimental methods, i.e., the Modified Layer Removal Method (MLRM) and Neutron Diffraction, to calculate peening and quenching stresses have been utilized in this work. The investigation was performed on thick Inconel 718 coatings on Inconel 718 substrates. Combined, these numerical and experimental techniques yield a deeper understanding of residual stress formation in the HVOF process and thus a tool for process optimization. The relationship between the stress state and deposit/substrate thickness ratio is given particular interest.

Keywords FEM simulation analysis, HVOF, Inconel 718, MLRM, neutron diffraction, residual stress, thick coating

1. Introduction

Thermally sprayed thick coatings have mainly been investigated in the perspective to form freestanding components. Less attention has been given to develop thick coatings for repair applications, which is of significant interest for the aerospace industry. One challenge when a coating several millimeters thick is to be sprayed is to control the residual stresses through the deposit thickness, and to understand the relationship between these stresses and coating adhesion. It is commonly known that coating adhesion and residual stress distribution are dependent on several factors such as pretreatment and process conditions during spraying and on post-treatment. In the present study, residual stress distribution of HVOF sprayed Inconel 718 coatings on Inconel 718 substrates has been investigated in order to understand the relationship between coating thickness and residual stresses.

1.1 Development of Residual Stresses

Residual stress is commonly defined as the stress that remains in a body that is not being subjected to external forces. It can be detrimental or beneficial to the performance of a material. Residual stresses in a component arise from mainly three different origins. Mechanically induced stresses are generated during manufacturing processes (such as grinding, blasting, and machining) and can produce nonuniform plastic deformation. Chemically induced stresses arise due to volume changes when chemical reactions, precipitations, or phase transformations occur during manufacturing. Thermally induced stresses are a consequence of nonuniform heating and cooling during manufacturing and processing. In a thermally sprayed coating, significant residual stresses can occur as a consequence of the high thermal and kinetic energies involved in the process and due to the difference in thermophysical and mechanical properties of substrate and coating materials. The stress distribution, its intensity and sign in the coating, is strongly dependent on the specific spray process (Ref 1) and processing conditions (Ref 2). Independent of the used process, coatings are subjected to a stress gradient at the coating-substrate interface. Compressive stresses are usually considered as beneficial increases with the in-flight particle velocity. The final residual stress state through the whole coating/substrate system is determined by superposition of stresses of different nature induced during the spray process: quenching, thermal mismatch, and peening stresses, together with the compressive stress state of the substrate induced during the gritblasting prior to spraying (Ref 3) (Fig. 1). Quenching stresses occur due to the rapid quenching of molten droplets when they solidify upon impact on the substrate or on the previous deposited layer. Thermal mismatch stresses occur during cooling but after solidification due to difference in thermal expansion coefficients between each deposited layer and the substrate material. In HVOF spraying significant peening stresses can occur due to high semimolten particle velocities (600 m/s), which are to be compared with plasma spraying

C. Lyphout and **P. Nylén**, University West, Trollhättan, Sweden; **A. Manescu**, Università Politecnica delle Marche, Ancona, Italy; and **T. Pirling**, Laue-Langevin Institute (ILL), Grenoble, France. Contact e-mail: christophe.lyphout@hv.se.

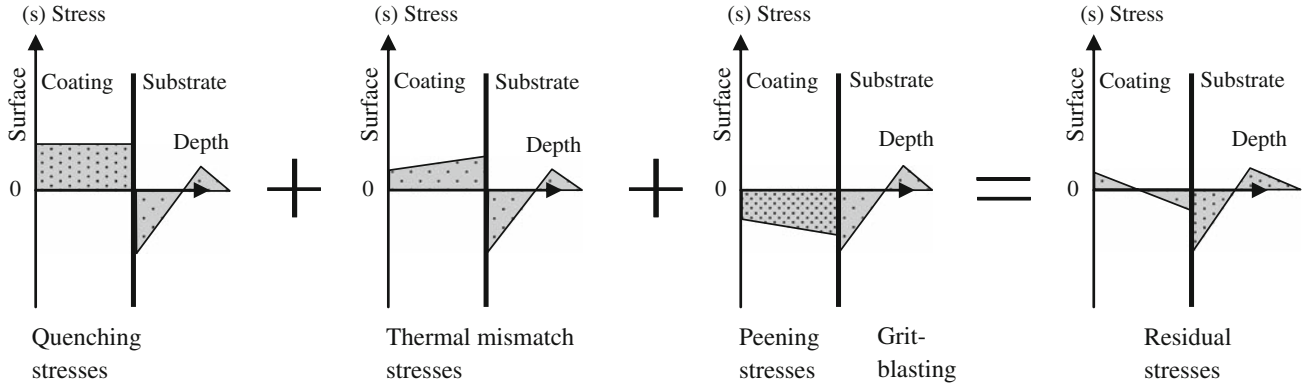

Fig. 1 Schematic representation of radial residual stress distribution in HVOF sprayed coating/substrate system

with corresponding velocities of 200 m/s and particles that are fully molten. The high particle velocity in HVOF spraying may cause a local plastic deformation resulting in local compressive stresses in the substrate as well as in the previous deposited layer. In a repair application the same material with almost identical composition as the substrate is sprayed. The small difference in thermal expansion coefficient between coating and substrate significantly reduces the contribution of the thermal mismatch stresses compared to quenching and peening stresses. The objective of this ongoing study is firstly to evaluate the final stress distribution using both numerical and experimental techniques and secondly to understand how coating thickness and process conditions affect the final stress state.

1.2 Effect of Residual Stresses on Coating Adhesion

The adhesion strength of a coating is dependent on the bonding between the coating and substrate as well as on the coating microstructure (Ref 4). Both the bonding and the microstructure are strongly influenced by residual stress distribution. It is commonly known that the level of residual stresses can significantly change at the coating substrate interface creating delaminations, which in worst cases can cause spallation. Compressive residual stresses at the interface are known to inhibit the formation of through-thickness cracks and to improve adhesion bonding (Ref 5). Stresses determination in thermal sprayed coatings has therefore been extensively studied. In situ monitoring of curvature (Ref 6) has been used to study the stress generation during coating formation. However, it is difficult to relate the in situ coating stress to the final residual stress state since both coating and substrate accommodate stresses during cooling. Godoy et al. (Ref 7) studied the change in curvature using the calculation methodology proposed by Clyne and Gill (Ref 5, 8). Even though the model was presented in the context of plasma sprayed coatings, adhesion strength was related to the shift between $\left(\Delta\sigma_{int}^{surf}\right)$ and $\left(\Delta\sigma_{int}^{S,C}\right)$, here adapted to HVOF coating according to Lesage et al. (Ref 9) (Fig. 2). $\left(\Delta\sigma_{int}^{surf}\right)$ Is the difference between the stress in the coating near the interface $\left(\sigma_{int}^{C}\right)$

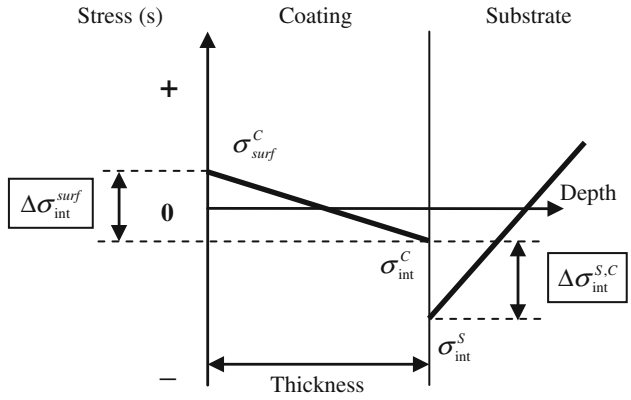

Fig. 2 Representation of radial residual stress distribution in HVOF system adapted from Lesage et al. (Ref 9)

and the stress at the surface $\left(\Delta\sigma_{surf}^{C}\right)$, and $\left(\Delta\sigma_{int}^{S,C}\right)$ is the difference between the stress in the coating near the interface $\left(\sigma_{int}^{C}\right)$ and the stress in the substrate near the interface $\left(\sigma_{int}^{S}\right)$. In the current study, such a model may provide a good framework to understand the relationship between the coating adhesion bond strength and the residual stress gap $\left(\Delta\sigma_{int}^{S,C}\right)$ at the coating-substrate interface.

2. Measurement of Residual Stresses

A number of techniques have been used in the past decades to measure residual stresses in thermal spray coatings (Ref 10). Limitations with these techniques occur when stress distributions in coatings several millimeters thick are of interest. Limitations also occur when identical materials are used for coating and substrate. A brief description of each method and its limitations for the current application is discussed below (Table 1).

2.1 Destructive Methods

Curvature measurement methods rely on the monitoring of changes in component distortion, either during

Table 1 Comparison of residual stress methods (Ref 10, 11)

Measurements techniques	X-ray diffraction	Neutron diffraction	Synchrotron diffraction	Layer removal
Strain state	Actual strain	Actual strain	Actual strain	Change in strain
Stress state	surface	volume	volume	Surface—volume
Depth profiling	Nondestructive	Nondestructive	Nondestructive	Destructive
Penetration	50 μm (Al); 5 μm (Ti)	200 mm(Al); 4 mm (Ti)	50 mm (Al)	Polishing step
Spatial resolution	1 mm lateral 20 μm in depth	0.5 mm	20 μm lateral 1 mm in depth	50 μm/removed layer
Accuracy	±20 MPa	±50 με	±10 με	±40 MPa

Table 2 HVOF process parameters, composition of the Amdry IN718 powder and IN718 mechanical properties

HVOF—Process parameters		Amdry—Powder							
Oxygen/Hydrogen ratio	0.5	Element	Ni	Cr	Mo	Fe	Ti	Al	Nb
Carrier gas flow rate, slpm	25	%, weight	53	19	3,0	18	0,9	0,5	5,1
Powder feeding rate, g/min	80	Properties	Substrate				Coating		
Spray distance, mm	230	E-modulus	200, GPa				120, GPa		
External cooling, slpm	360	Poisson's ratio	0.30				0.25		

deposition (in situ) or after (postmortem) by successively removing material to allow relaxation of the stresses (Ref 11). In the latter, layers are removed by polishing one side of the specimen; then the stresses become unbalanced and the specimen bends. For coatings, the method is based on the same basic principles as the layer removal technique, usually called Modified Layer Removal Method (Ref 12, 13), which is further described in section 2.2.1 beneath, where strains of successively deposited layers are recorded. The major limitation with this method is that stresses might be induced during polishing.

2.2 Nondestructive Methods

Diffraction methods are based on the elastic deformations within a polycrystalline material to measure internal stresses in a material (Ref 14, 15). The stresses cause deformation i.e., changes in the distance between the lattices, which are used as internal strain gages. Shifts in diffraction peaks are recorded from which the strain distribution is calculated.

2.2.1 X-Ray Stress Evaluation (XSE). The penetration depth of low-energy X-Ray Diffraction using a traditional Kα-Cu radiation wavelength is limited to a few tens of micrometers, depending on the investigated material. Although X-ray scattering offers a high spatial resolution, analyzed thickness is not high enough to cover the depth of thick thermally sprayed coatings. Such a surface diffraction method is more dedicated to surfaces and interfaces structural characterization.

2.2.2 Neutron Diffraction. Compared to low-energy X-rays the main advantage of working with neutrons is the possibility to analyze greater depths, i.e., higher coating thicknesses. Neutrons have the following advantage over X-ray photons: for wavelengths comparable to the atomic spacing, their penetration into engineering materials is in the range of several millimeters, due to their interaction only with nuclei instead of electrons.

2.2.3 High-Energy X-ray Diffraction. High-energy photons using synchrotrons radiation offer the possibility for combining a high penetration power similar to neutron diffraction with the high resolution reached with X-ray scattering. The resulting scattered intensities require smaller correction factors since extremely small diffracted angles are measured, compared to neutron diffraction.

All of these diffraction techniques use the same methods to determine the shift in diffracted peaks to compute strain distribution. Residual stress calculation relies on mechanical properties of both bulk and coating material, and the determination of the unstressed lattice parameter d_0, which can be difficult to determine from the coating material since the particulate feedstock is sprayed.

3. Experimental Procedure

3.1 Spraying Process

Inconel 718 powder was deposited on Inconel 718 substrate using a Sulzer-Metco HVOF hybrid DJ-2600 gun. Oxygen/hydrogen gases were chosen as the oxy-fuel mixture. HVOF parameter settings are listed in Table 2. The substrates used were Inconel 718 coupons with dimensions of 25.4 mm in diameter 3 mm thickness. Substrates were degreased and gritblasted according to usual standard procedures prior to coating deposition. The gritblasted substrates had a mean roughness (Ra) of 2.5 μm. A series of four sets of three specimens each were coated to 1.0, 1.5, 2.0, and 2.5 mm (±40 μm) thickness. Both the Neutron Diffraction method and the Modified Layer Removal Method were utilized.

3.2 Coating Characterization

3.2.1 Destructive methods. The Modified Layer Removal Method was used to determine the through-thickness

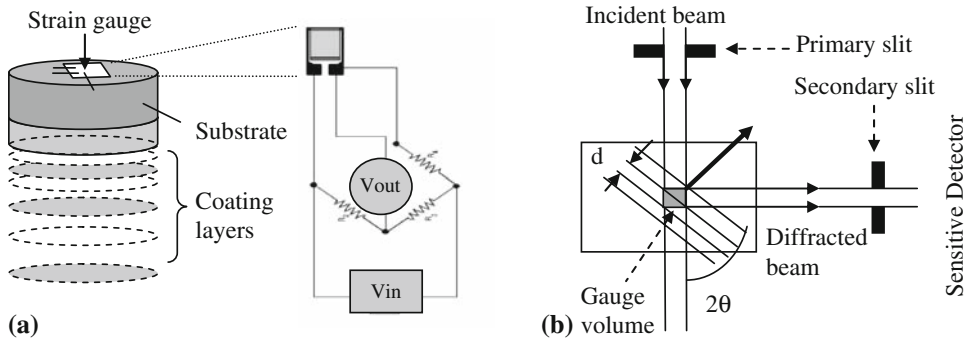

Fig. 3 (a) Modified layer removal method; (b) Neutron diffraction method

residual stress distribution in the coating. The procedure involved gluing a strain gage to the uncoated side of the specimen and then measuring the strain change after removing successive layers by mechanical polishing (Fig. 3a). Diamond particles (9 μm) were used under a constant force of 135 N to remove the material thickness from 20 to 100 μm in each polishing step. Strain and thickness changes were recorded simultaneously as layers were removed, and used for the residual stress determination using the back-computation procedure (Ref 13, 16). Material properties are given in Table 2. Previous studies revealed that the longitudinal and transverse strains were similar, measured via a 90° rosette gage. Therefore, three-wire strain gages were used.

3.2.2 Nondestructive Methods. Neutron Diffraction measurements were carried out at the Hahn-Meitner Institute (HMI) facility located in Berlin, and at the ILL SALSA reactor facility in Grenoble. A monochromatic neutron beam of a cross section of 0.6×0.6 mm^2 was used for residual strain measurements at room temperature, in a spatially resolved mode (Fig. 3b). The Bragg peaks (220) and (111) for Ni-alloy were measured to $2\theta = 86°$ and 47°, using a wavelength (λ) of 0.147 and 0.165 nm, respectively. From the obtained diffracted peaks, the lattice spacing d_{hkl} (where h, k, and l stand for Millers indices of the investigated lattice plane) was evaluated using Bragg's law (Eq. 1) with the corresponding lattice strain (Eq. 2) defined as a function of the "stress free" lattice parameter d_0.

$$\lambda = 2\, d_{hkl} \sin\theta \qquad \text{(Eq 1)}$$

$$\varepsilon_{hkl} = (d_{hkl} - d_0)/d_0 \qquad \text{(Eq 2)}$$

The d_0 values for both deposit and substrate were obtained by balancing the stress, respectively, through a freestanding coating and an annealed gritblasted substrate. Considering the deposition method, measurements were performed only in radial and axial directions, by scanning the sample from the top to the bottom (Fig. 4), using, respectively, the reflection and transmission modes. Corresponding residual stresses were calculated using Eq. 3 and 4 for isotropic Hookean elasticity:

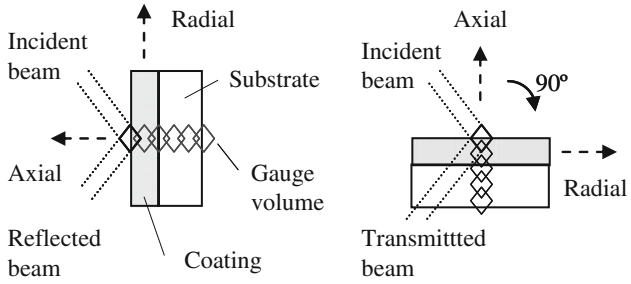

Fig. 4 Reflection and transmission measurement modes

$$\sigma_{11} = \frac{E}{(1+\nu)(1-2\nu)}[\varepsilon_{11} + \varepsilon_{33}] \qquad \text{(Eq 3)}$$

$$\sigma_{33} = \frac{E}{(1+\nu)(1-2\nu)}[2\nu\varepsilon_{11} + (1-\nu)\varepsilon_{33}] \qquad \text{(Eq 4)}$$

3.2.3 Finite Element Analysis. The current ongoing work concerns the development of a finite element (FE) methodology to simulate residual stresses generated in a HVOF coating and substrate system. Preliminary studies on a layer deposition model have been investigated to predict the quenching and thermal mismatch stresses. However, to implement peening stresses into the layer deposition model, the thermomechanical process associated with particle impingement has to be first investigated. The impact of a single particle has been extensively studied using FE modeling for the shot-peening process (Ref 17), and recently extended to simulate the peening contribution of particles impingement during HVOF spraying, using a finite element code ABAQUS (Ref 18, 19). In the present study, the capability of the solid-mechanic Msc.Marc® software was evaluated. The impact of an IN718 solid single particle just below its melting temperature was modeled to predict the peening stresses induced in the radial and axial direction of an IN718 substrate. The impact was defined as a nonlinear dynamic contact event, and studied via a thermomechanical coupled dynamic transient analysis.

A two-dimensional axisymmetric model of a 50 μm diameter particle impacting on a substrate disc of 0.2 mm in radius and 0.2 mm in depth was developed (Fig. 5a). Temperature dependence of the plasticity model obtained from experimental data (Ref 20) was considered (Fig. 5b). In a first approach, a constant strain rate of 10 s^{-1} was considered, keeping in mind that the real rapid impact may lead to a higher and time dependent strain rates. Temperature dependence of specific heat, thermal conductivity, thermal expansion coefficient, and Young's Modulus were also considered (Ref 20). Large deformations at the interface were accommodated using quadratic elements and an adaptative local mesh refinement, based on maximum curvature control. Contact between the impacting particle and the target substrate was controlled by a Coulomb friction model, assuming a friction coefficient of 0.5, which was also compared with maximal friction using a glue contact. The heat transfer at the interface was controlled by introducing a thermal contact resistance of 10^{-7} m^2 K/W. Particle velocities of 500 m/s and 600 m/s were evaluated with a particle temperature of 1270 °C, just below its melting point.

4. Results and Discussion

4.1 Modified Layer Removal Method (MLRM)

Increasing the coating thickness from 1 to 2.5 mm did not significantly change the residual stress level through the coating thickness (Fig. 6a). The profile exhibited a succession of negative and positive low stress values along the coating thickness; resulting from local accommodation between each deposited layer of the different nature of stresses issued while spraying. The top of each coating displayed tensile stresses whereas stresses of compressive nature remained at the interface. High compressive stresses were found at the interface in both coating and substrate, and these stresses rapidly changed into tensile stresses within the first hundred microns of the substrate. The compressive stress amplitude of the substrate at the interface decreased from 420 to 215 MPa for the coating thicknesses 1 and 2.5 mm (Fig. 6a). Continuity of compressive stresses at the coating/substrate interface transfers the stress accommodation from the interface to the first hundreds microns of the substrate itself. A decrease

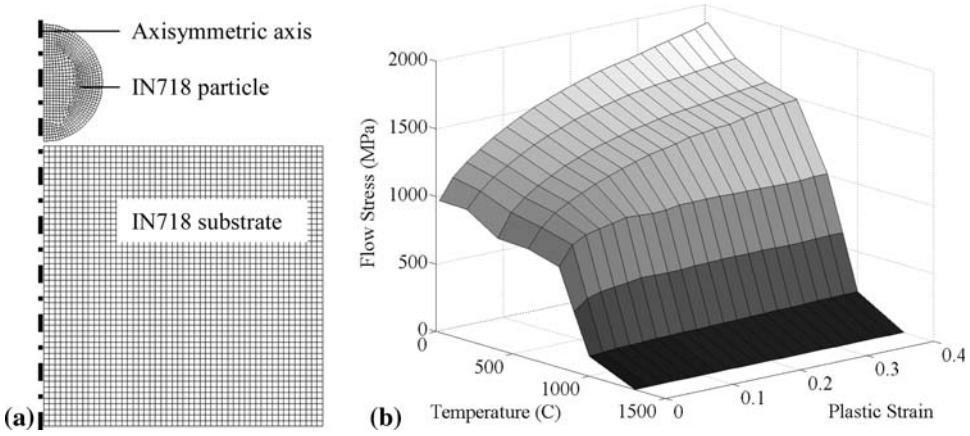

Fig. 5 (a) Axisymmetric model of an IN718 particle impacting on an IN718 substrate; (b) Temperature dependent stress-strain relationship for a 10 s^{-1} strain rate (Ref 20)

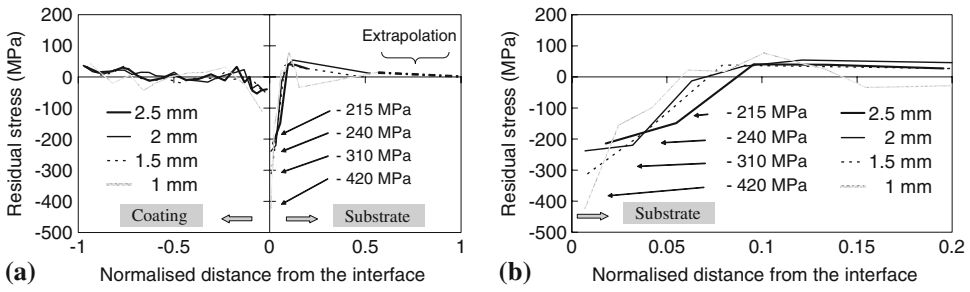

Fig. 6 MLRM radial residual stresses profiles through thick coatings deposited on 3 mm thick substrates

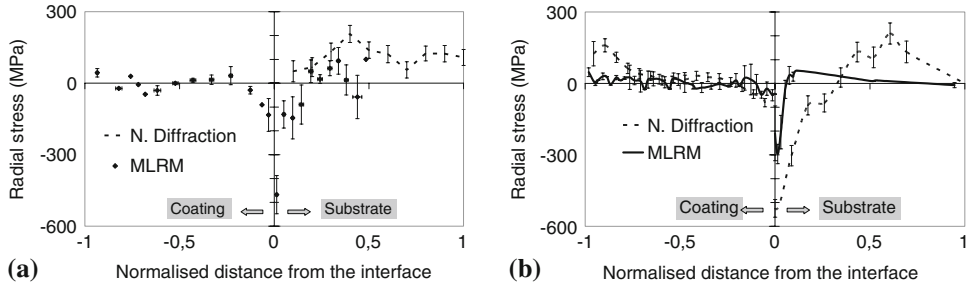

Fig. 7 Radial residual stress profiles through: (a) 1 mm thick coating on 3 mm substrate—HMI,Berlin; (b) 2 mm thick coating on 3 mm substrate—ILL, Grenoble

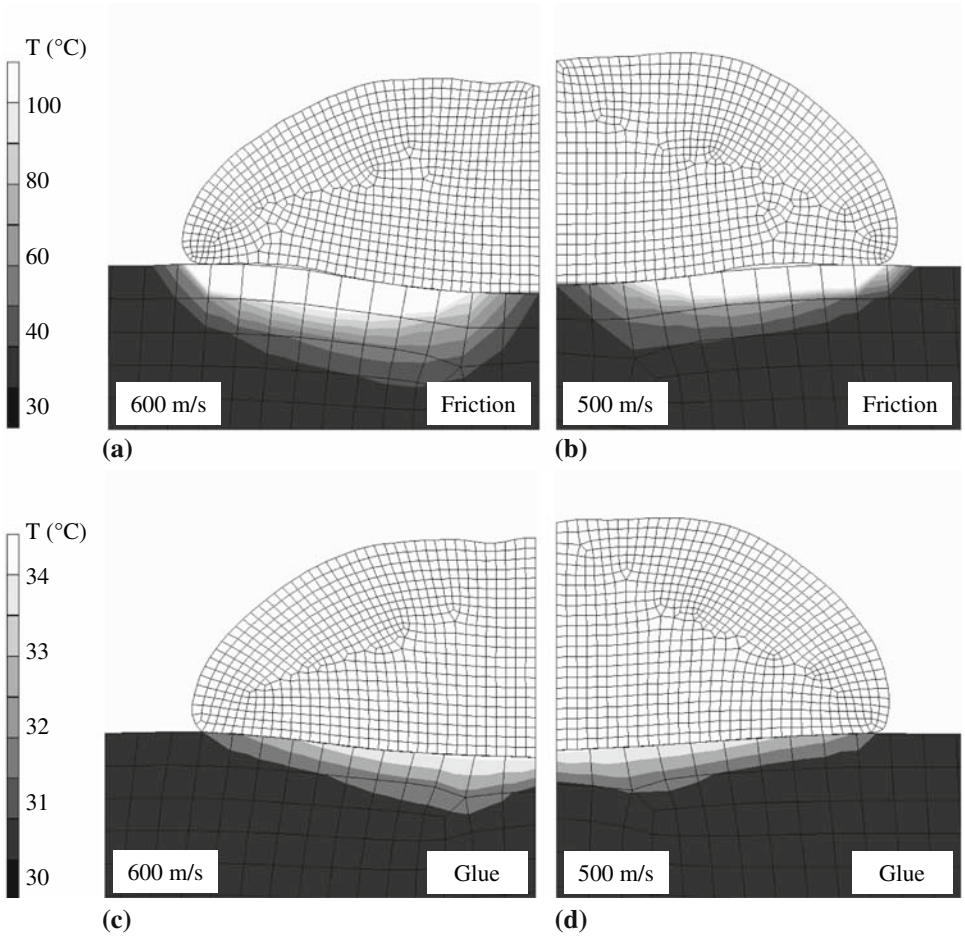

Fig. 8 Temperature distribution through the particle/substrate system after reaching a flattening time of 0.1 μs and before cooling starts. Contact friction model after impact at (a) 600 m/s and (b) 500 m/s; contact glue model after impact at (c) 600 m/s and (d) 500 m/s

of the stress gap at the coating-substrate interface $\left(\Delta\sigma_{int}^{S,C}\right)$ for increased coating thickness can be seen in Fig. 6(b). The hypothesis of heat effect as stress relief mechanism at the interface will be investigated in future work. It should be noted that the tensile strength has been previously measured above 80 MPa (Ref 21) for all coating thicknesses.

4.2 Neutron Diffraction Method (ND)

The experiments carried out at the HMI institute in Berlin allowed analyses of only stress profiles in the substrate (Fig. 7a). From this experimental setup, the Ni-(220) diffraction peak was analyzed. The corresponding diffraction angle close to 90º gave high spatial resolution, but not enough signal intensity to measure the

broader peaks of the coating. To gain in response intensity, the Ni-(111) most intense peak was considered in the experimental work carried out at the ILL Institute in Grenoble. The full coating/substrate system was scanned (Fig. 7b). Good agreement was found between these results and the MLRM ones with regard to the ''stress-free'' profile through the coating thickness. However, interface measurements, which superimpose both coating and substrate contribution, resulted in overestimating the local compressive stresses in the vicinity of the interface (±0.2 mm). It has to be noted that the resolution near the coating-substrate interface was highly affected by the relatively large sampling volume. Therefore, the stress level in this region has to be considered as uncertain. The development of a new deconvolution procedure, based on modeling the Gaussian-like distribution of the intensity through the gage volume, may increase the resolution in this region. This will be considered in future work.

4.3 Finite Element Analysis

The previous experimental results with low stress levels in the coating compared to corresponding levels at the coating-substrate interface initiated modeling work to simulate the stresses in this region. Initial simulations with a layer by layer model indicated that the major stress components in the current applications are quenching and peening stresses, the reason why it was decided to concentrate the work to modeling of single particle impacts. The deformed shape of flattened particles, impacting over the target substrate with two different velocities, is presented in Fig. 8. The flattening degree, commonly defined as the radius ratio of the final splat to the initial particle, increased from 1.48 to 1.60 for the corresponding particle velocities of 500 and 600 m/s, independent of the contact model used. The flattening time of the particle ($t_f < 0.1$ μs), defined as the time needed for the impinging particle to reach its final diameter after impact, was found to be significantly shorter than the solidification time, as it has been already reported by Fan et al. (Ref 22). When considering the glue contact model, the heat transfer from particle to substrate during the flattening time was controlled by conduction (Fig. 8c, d). In comparison the introduction of a friction model generated heat into the substrate subsurface during the flattening period at each location point where the contact was initiated (Fig. 8a, b). The heat flux generated by friction increased with the particle kinetic energy. The model predicted axial compressive stress levels in the range of 500 MPa, up to 20 microns in the substrate depth, which implies a dominant contribution of the particle momentum to the axial stresses (Fig. 9a). However, the predicted radial residual stress amplitude exceeds the yield strength of the material (1040 MPa) with unrealistically 80% in the radial direction, when the particle impacts at 600 m/s (Fig. 9b). Such radial distribution is not representative of any physical bonding since the contact is numerically controlled by imposing a constant Coulomb friction coefficient of 0.5. However, these results are comparable with those obtained from shot peening of strain-hardening materials (Ref 23). In the case of a fully molten droplet, assuming a negligible vaporization of the in-flight particle, its momentum may introduce the same order of axial compressive stresses in the substrate. However, the kinetic

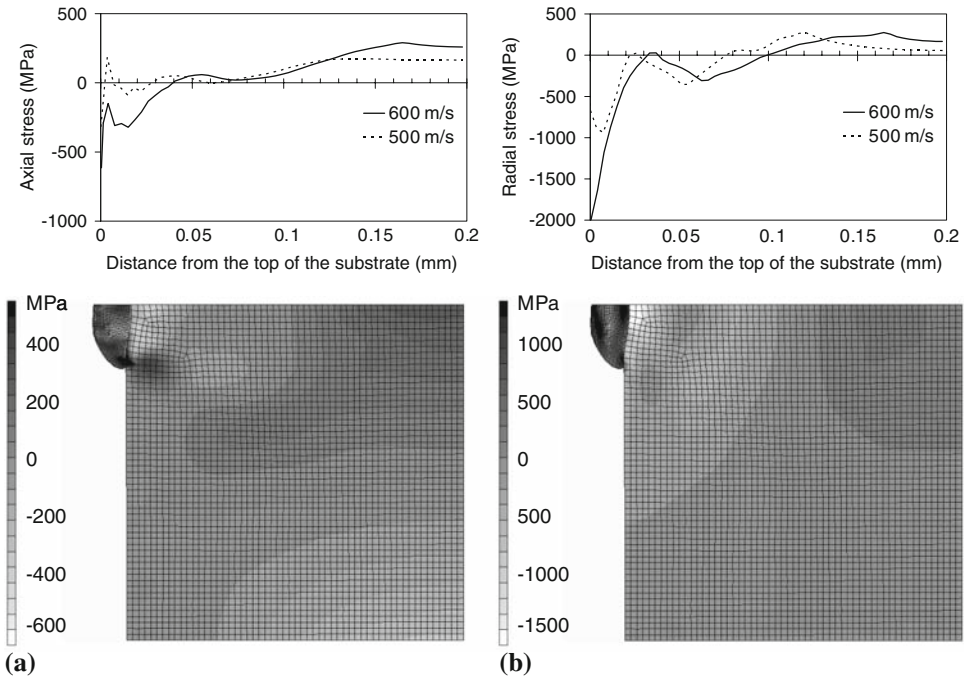

Fig. 9 (a) Axial and (b) radial residual stress distribution along the centerline and through the particle-substrate system, after impact of a single solid particle at 600 m/s

energy may be radially redistributed, since the contact may be essentially influenced by the liquid properties, such as surface tension and wetting angle, lowering both interfacial friction and radial compressive stresses.

5. Summary and Conclusion

Residual stress distributions in HVOF sprayed Inconel 718 coatings on Inconel 718 substrates have been investigated. The purpose with the ongoing study is to gain a deeper understanding of residual stress formation in thick coatings through experimental and modeling techniques. The main results can be briefly summarized:

- Increasing the coating thickness seems not to modify the residual stress distribution through the coating, and corresponding stress values have to be considered as low for all coating thicknesses.
- Compressive stress is achieved both in coating and in substrate at the interface, but the difference in stress amplitude at the interface $\left(\Delta\sigma_{\text{int}}^{\text{S,C}}\right)$ seems to significantly decrease when coating thickness is increased. These compressive stresses may be the reason for the good bonding of the coatings, which was measured to be above 80 MPa for all thicknesses in previous work.
- The Neutron Diffraction method needs to be further developed to be capable of determining the stress levels in the specific coating/substrate system and thicknesses used in this study. Examples of necessary developments are:
  - development of a reliable deconvolution procedure at the interface to distinguish between the two superimposed diffraction peaks, since both coating and substrate materials are Ni-based alloys.
  - a precise method to determine the unstressed lattice plane parameter d_0 for this specific material.
- The capability to predict peening and quenching stresses by the software MSC. Marc that utilizes thermo-mechanical coupled analysis with remeshing was demonstrated by simulating single particle impacts. The model is to be extended to predict thermal mismatch stresses through a multilayer deposition model.

Acknowledgments

The authors acknowledge the financial support of the VINNOVA (Swedish Governmental Agency for Innovation Systems) funded NFFP project and the technical support of the Thermal Spray Department of Volvo Aero Corporation (Trollhättan, Sweden). The research project has been supported by the EC under the 6th Framework Programme through the Key Action: Strengthening the European Research Area, Research Infrastructures. Contract no.: RII3-CT-2003-505925 (NMI3). The authors would like to thank Dr. R. Wympory and Dr. D.J. Hughes for their respective collaboration to carry out Neutron Diffraction measurement at the Hahn-Meitner Institute (Berlin) and at the Laue-Langevin Institute (Grenoble). Particular acknowledgments are addressed to Kjell Niklasson of University West (Trollhättan) for supervision in the FEA simulations.

References

1. S. Sampath, Y.Y. Jiang, J. Matejicek, L. Prchlik, A. Kulkarni, and A. Vaidya, Role of Thermal Spray Processing Method on the Microstructure, Residual Stress and Properties of Coatings: An Integrated Study for NiAl Bond Coats, *Mater Sci. Eng.*, 2004, **364**(1-2), p 216-231
2. J. Matejicek, S. Sampath, D. Gilmore, and R. Neiser, In Situ Measurement of Residual Stresses and Elastic Moduli in thermal sprayed Coatings—Part 2: Processing Effects on Properties of Mo Coatings, *Acta. Mater.*, 2003, **51**, p 873-885
3. C.R.C. Limaa, J. Ninb, and J.M. Guilemany, Evaluation of residual stresses of thermal barrier coatings, *Surf. Coat. Technol.*, 2006, **200**, p 5963-5972
4. M. Ohring, *Materials Science of Thin Films, Deposition and Structures*, Academic Press, 2002
5. T.W. Clyne and S.C. Gill, Residual Stresses in Thermal Spray Coatings and Their Effect on Interfacial Adhesion: a Review of Recent Work, *J. Therm. Spray Tech.*, 1996, **4**, p 401-409
6. R. Moltz, A. Valarezo, and S. Sampath, Comparison of Coating Stresses Produced by High Velocity Liquid/Gas Fuel and Triplex 200 Plasma Processes Using In-Situ Coating Stress Measurement, *Proceedings of the ITSC 2008*, Maastricht, Netherlands, 2008, p 473-478
7. C. Godoy, E.A. Souza, M.M. Lima, and J.C.A. Batista, Correlation Between Residual Stresses and Adhesion of Plasma Sprayed Coatings: Effects of a Post-Annealing Treatment, *Thin Solid Films*, 2002, **420-421**, p 438-445
8. S.C. Gill and T.W. Clyne, Investigation of Residual Stress Generation During Thermal Spraying by Continuous Curvature Measurements, *Thin Solid Films*, 1994, **250**, p 172-180
9. P. Araujo, D. Chicot, M. Staia, and J. Lesage, Residual Stresses and Adhesion of Thermal Spray Coatings, *Surf. Eng.*, 2005, **21**, p 35-40
10. P.J. Withers and H.K.D. Bhadeshia, Residual Stress—Measurement Techniques, *Mater. Sci. Technol.*, 2001, **17**, p 355-365
11. F.A. Kandil, J.D. Lord, A.T Fry, and P.V. Grant, *A Review of Residual Stress Measurement Methods*, NPL Materials Centre, report MATC(A)04, 2000
12. ASM International-TSS. Accepted Practice Mechanical Properties # 1-AP MP001-02 Modified layer Removal Method for Evaluating Residual Stresses in Thermal Spray Coatings, ASM-TSS, Materials Park, OH, USA, 2002, p 25
13. D.J. Greving, E.F. Rybicki, and J.R. Shadley, Through-Thickness Residual Stress Evaluation for Several Industrial Thermal Spray Coatings Using a Modified Layer-Removal Method, *J. Therm. Spray Tech.*, 1994, **3**(4), p 379-388
14. J. Pina, A. Dias, and J.I. Lebrun, Study by X-Ray Diffraction and Mechanical Analysis of the Residual Stress Generation During Thermal Spraying, *Mater. Sci. Eng.*, 2003, **A347**, p 21-31
15. T.C. Totemeier, R.N. Wright, and W.D. Swank, Residual Stresses in High-Velocity Oxy-Fuel Metallic Coatings, *Metall. Mater. Trans.*, 2004, **35A**, p 1807-1814
16. R.T.R. McGrann, E.F. Rybicki, and J.R Shadley, Applications and Theory of the Modified Layer Removal Method, *Proceedings of the Fifth ICRS*, Linköping, Sweden, June 16-18, 1997
17. S.A. Meguid, G. Shagal, and J.C. Stranart, Finite Element Modelling of Shot-Peening Residual Stresses, *J. Mater. Process. Tech.*, 1999, **92-93**, p 401-404
18. K. Yokoyama, M. Watanabe, S. Kuroda, Y. Gotoh, T. Schmidt, and F. Gärtner, Simulation of Solid Particle Impact Behavior for Spray Processes, *Mater. Trans.*, 2006, **47**(7), p 1697-1702

19. P. Bansal, P.H. Shipway, S.B. Leen, *Acta Materialia*, 2007, **55**, 5089-5101
20. Internal Report, Volvo Aero Corporation
21. C. Lyphout, P. Nylén, and J.Wigren, Characterization of Adhesion Strength and Residual Stress of HVOF sprayed Inconel 718, *Proceedings of the ITSC 2007*, Beijing, China, 2007, p 588-593
22. Q. Fan and L. Wang, Modelling of Temperature and Residual Stress Fields, *Proceedings of the ITSC 2005*, Basel, Switzerland, 2005, p 275-279
23. T. Hong et al., A Numerical Simulation to Relate the Shot Peening Parameters to the Induced Residual Stresses, *Eng. Fail. Anal.*, 2008, **15**, p 1097-1110